THE JOURNAL OF BIOLOGICAL CHEMISTRY VOL. 280, NO. 52, pp. 42952–42959, December 30, 2005

The $P2X_7$ Nucleotide Receptor Mediates Skeletal Mechanotransduction*

Received for publication, June 13, 2005, and in revised form, September 29, 2005 Published, JBC Papers in Press, November 3, 2005, DOI 10.1074/jbc.M506415200

Jiliang Li[‡1], Dawei Liu[§1], Hua Zhu Ke[¶], Randall L. Duncan[§], and Charles H. Turner[§‖2]

From the [‡]Department of Anatomy and Cell Biology and [§]Department of Orthopaedic Surgery, Indiana University School of Medicine, Indianapolis, Indiana 46202, the [¶]Pfizer Global Research and Development, Groton Laboratories, Groton, Connecticut 06340, and the [‖]Biomechanics and Biomaterials Research Center, Department of Biomedical Engineering, Indiana University-Purdue University Indianapolis, Indianapolis, Indiana 46202

The $P2X_7$ nucleotide receptor ($P2X_7R$) is an ATP-gated ion channel expressed in many cell types including osteoblasts and osteocytes. Mice with a null mutation of $P2X_7R$ have osteopenia in load bearing bones, suggesting that the $P2X_7R$ may be involved in the skeletal response to mechanical loading. We found the skeletal sensitivity to mechanical loading was reduced by up to 73% in $P2X_7R$ null (knock-out (KO)) mice. Release of ATP in the primary calvarial osteoblasts occurred within 1 min of onset of fluid shear stress (FSS). After 30 min of FSS, $P2X_7R$-mediated pore formation was observed in wild type (WT) cells but not in KO cells. FSS increased prostaglandin (PG) E_2 release in WT cells but did not alter PGE_2 release in KO cells. Studies using MC3T3-E1 osteoblasts and MLO-Y4 osteocytes confirmed that PGE_2 release was suppressed by $P2X_7R$ blockade, whereas the $P2X_7R$ agonist BzATP enhanced PGE_2 release. We conclude that ATP signaling through $P2X_7R$ is necessary for mechanically induced release of prostaglandins by bone cells and subsequent osteogenesis.

Mechanical loads applied to bone tissue increase bone formation and improves bone strength (1). Previous studies have suggested that several osteogenic factors, including insulin-like growth factors, transforming growth factor-β, nitric oxide (NO), and prostaglandins (PGs),[3] mediate mechanically induced bone formation (2–5). PGs in particular have been intensively investigated. Numerous cell culture studies have demonstrated an increased production of PGs in osteoblasts and osteocytes subjected to fluid shear stresses (for review, see Ref. 6). Several PGs have independent anabolic effects on bone tissue. In particular PGE_2 greatly enhances the synthetic activities of osteoblasts (7).

In addition to PGs, nucleotides, such as ATP and UTP, are released from cells in response to mechanical stimulation (8–11), including osteoblasts (12, 13). These nucleotides can act as autocrine and paracrine factors through activation of purinergic (P2) receptors. Both osteoblasts and osteoclasts express several types of P2 receptors (for review, see Ref. 14). Activation of P2 receptors in bone cells by ATP has been shown to increase $[Ca^{2+}]_i$ (15, 16). P2 signaling also modulates cyclo-oxygenase-2 expression (17), PG release (18, 19), and c-*fos* expression (20) in osteoblasts and other cell types.

Based on their molecular structure and activated signal pathways, P2 purinergic receptors are divided into two classes: P2X and P2Y (21). The P2X receptors are ligand-gated ion channels that, in general, are nonselective for monovalent cations. However, some of these receptors are also permeable to Ca^{2+} or even anions. P2Y receptors are G protein-linked receptors that in many cases are coupled through phospholipase C to the release of Ca^{2+} from intracellular stores. Seven P2X subtypes and six P2Y subtypes have been identified in mammalian cells (22). The $P2X_7$ receptor ($P2X_7R$) appears to be the most divergent member among P2X family. $P2X_7Rs$ have the unique ability to form large aqueous pores in the membrane, permeable to hydrophilic molecules as large as 900 Da with prolonged exposure to agonists (21). Activation of $P2X_7Rs$ stimulates the release of the inflammatory cytokines such as interleukin-1β in immune cells (23). $P2X_7R$ activation also results in cell membrane blebbing (24) and changes in cellular morphology, which eventually leads to cell death by both necrotic and apoptotic mechanisms (25).

The $P2X_7R$ forms a complex with several proteins including β2 integrin, receptor-like tyrosine phosphatase (RPTP), α-actinin, phosphatidylinositol 4-kinase, membrane-associated guanylate kinase, and several heat shock proteins (26). Several of these proteins are associated with mechanotransduction. For instance, RPTP is involved in force-dependent formation of focal adhesion complexes (27), and α-actinin links β integrins with the actin cytoskeleton promoting transduction of mechanical forces (28). Recently, mice with a null mutation of the $P2X_7R$ were shown to have reduced total bone mineral content, smaller periosteal circumference in the femur, increased trabecular bone resorption, and reduced periosteal bone formation (29). This phenotype of suppressed periosteal bone formation coupled with increased trabecular bone resorption resembles the effects of disuse on the skeleton. When a weight-bearing limb is placed in disuse, *e.g.* with a plaster cast, periosteal bone formation is suppressed and trabecular bone resorption increases (30). Considering the nature of the protein complex interacting with $P2X_7R$ and the observation that $P2X_7R$ null mice resemble the skeletal disuse phenotype, we hypothesized that the $P2X_7R$ may be necessary for the proper skeletal response to mechanical loading.

To answer the question whether mice lacking the $P2X_7R$ have decreased skeletal sensitivity to mechanical loading, we measured the skeletal response to loading in $P2X_7R$ knock-out (KO) mice. To further study the role of $P2X_7R$ in the osteoblastic response to mechanical loading, calvarial cells isolated from newborn KO and wild type (WT) mice were subjected to a steady laminar fluid flow (FSS). We found that 30 min FSS increased the cellular uptake of 4-[(3-methyl-2(3H)-benzoxazolylidene)methyl]-1[3-(trimethylammonio)propyl]iodide (YO-PRO-1) (molecular mass = 630 daltons) mediated by $P2X_7R$ mediated pore formation in WT

* This work was supported by National Institutes of Health Grants R01AR046530 (to C. H. T.), RO1AR43222 (to R. L. D.), and P01AR045218 (to R. L. D.). The costs of publication of this article were defrayed in part by the payment of page charges. This article must therefore be hereby marked "*advertisement*" in accordance with 18 U.S.C. Section 1734 solely to indicate this fact.

[1] Both of these authors contributed equally.

[2] To whom correspondence should be addressed. Tel.: 317-274-3226; Fax: 317-274-3702; E-mail: turnerch@iupui.edu.

[3] The abbreviations used are: PG, prostaglandin; $P2X_7R$, $P2X_7$ nucleotide receptor; RPTP, receptor-like tyrosine phosphatase; KO, knock-out; FSS, fluid shear stress; WT, wild type; PBS, phosphate-buffered saline; MEM, α-minimal essential medium; FBS, fetal bovine serum; BzATP, 2′,3′-*O*-(4-benzoyl)benzoyl-ATP; BBG, Brilliant Blue G; YO-PRO1, 4-[(3-methyl-2(3H)-benzoxazolylidene)methyl]-1[3-(trimethylammonio-)propyl]iodide; TNF, tumor necrosis factor; CHX, cyclohexamide; Cx43, connexin 43.

cells but not in KO cells. Application of FSS for 15–60 min significantly increased PGE_2 release in WT cells but not in KO cells. In addition, we demonstrated that mechanical signals induced ATP signaling in MC3T3-E1 osteoblasts and MLO-Y4 osteocytes and that ATP activation of $P2X_7$ is necessary for the subsequent release of PGE_2.

EXPERIMENTAL PROCEDURES

Animals—The $P2X_7R$ KO mouse was generated as reported by Solle *et al.* (31). The $P2X_7R$ KO ($P2X_7R^{-/-}$) mice as well as the WT ($P2X_7R^{+/+}$) mice (C57BL/6) were purchased from Taconic (Germantown, NY) at 4–5 weeks of age. The animals were housed at Indiana University School of Medicine Animal Care Facility for 13–14 weeks (acclimation period) before the experiment began. All animals were allowed free access to standard mouse chow and water during the whole experimental period. All procedures performed were in accordance with the Indiana University Animal Care and Use Committee Guidelines.

In Situ Mechanical Properties of the Ulna and Radius—When the animals reached 18 weeks of age, five mice from male and female WT and KO mice were chosen at random, anesthetized and killed by cervical dislocation. Immediately after killing, each animal was weighed, and the forearm was tested using a miniature materials testing machine (Vitrodyne V1000; Liveco, Inc., Burlington, VT), which has a force resolution of 0.05 newton. The right arm was minimally dissected to expose the medial surface of the midshaft ulna. A single element strain gauge (model EA-06–015DJ-120; Measurements Group, Inc., Raleigh, NC) was fixed to the exposed medial ulnar surface with cyanoacrylete (M-Bond 200; Measurements Group, Inc.) at a point 3.35 mm distal to the brachialis insertion based on the previous report in our laboratory (32). Once fitted with a strain gauge, the voltage was zeroed, and the forearm was loaded in cyclic axial compression using an electromagnetic actuator with force feedback control. Using a 2-Hz haversine waveform, the forearms were laded at 0.95, 1.40, 1.85, and 2.3 newtons, during which peak-to-peak voltage was measured on a digital oscilloscope. Voltage measurements were converted to strain as reported previously (32).

In Vivo Ulnar Loading—Animals in each gender WT or KO mice were subdivided randomly into 3 groups for *in vivo* loading: low magnitude, medium magnitude, or high magnitude loading groups. Under anesthesia with inhalation of isoflurane (2%), the right forearm of each mouse was loaded at 120 cycles per day for 3 consecutive days with a 2-Hz haversine waveform using the electromagnetic actuator. The left forearms were not loaded and served as an internal control for loading effects. All mice were allowed normal cage activity between loading sessions and afterward. Intraperitoneal injections of calcein (30 mg/kg body weight; Sigma) and alizarin (50 mg/kg body weight; Sigma) were administered 5 and 11 days after the first loading day. All animals were killed 18 days after the first loading day.

Tissue Processing, Histomorphometry, and Ulnar Strain Calculations—Right and left ulnae were processed as reported previously (32). Transverse thick sections (70 μm) were cut at the ulnar midshaft and further ground to a final thickness of 20 μm and then mounted unstained on microscope slides. One section per limb was read on a Nikon Optiphot flurescence microscope (Nikon, Inc., Garden City, NJ) using the Bioquant digitizing system (R&M Biometrics, Nashville, TN). The following primary data were collected from the periosteal surface at $\times$250 magnification: total perimeter (B.Pm); single label perimeter (sL.Pm); double label perimeter (dL.Pm), and double label area (dL.Ar). From these primary data, the following derived quantities were calculated: mineralizing surface (MS/BS = [1/2sL.Pm + dL.Pm]/B.Pm $\times$100; %); mineral apposition rate (MAR = dL.Ar/dL.Pm/6 days; μm/day) and bone formation rate (BFR/BS = MAR $\times$ MS/BS $\times$ 3.65; $\mu m^3/\mu m^2$ per year). A new set of relative (r) values: rMS/BS, rMAR, and rBFR/BS using the left ulna (nonloaded) values subtracted from the right ulna (loaded) values showed purely mechanically induced bone formation.

Each ulnar cross-section used for histomorphometry was digitally captured through the microscope and imported into SCIONIMAGE, in which total area (Tt.Ar; mm^2), cortical area (Ct.Ar; mm^2), maximum second moment of inertia (I_{MAX}; mm^4); I_{MIN} and Se.Dm were calculated. Mechanical strain was calculated for the medial periosteal surface of each histological section using methods described in Robling and Turner (32).

Cell Culture—Calvarial osteoblasts were obtained from 3–5-day-old neonatal calvariae from WT and KO mice. Calvariae halves of the same genotype were grouped and subjected to four sequential 20-min digestions with enzyme mixture of 1.5 units/ml collagenase (Sigma) in PBS and 0.05% trypsin, 1 mM EDTA (Invitrogen) at room temperature on a rocking platform. The first digest was discarded. The second to the fourth digest were pooled, and cell pellet was collected after centrifugation at 2,000 rpm for 10 min. Cells were resuspended in α-minimal essential medium (α-MEM) and passed through a 40-μm cell strainer (Falcon, BD Biosciences). Cell numbers were counted, and cells were plated at an initial density of 2,000 cells/cm^2 in a T25 culture flask (Costar, Corning, NY) in α-MEM containing 10% fetal bovine serum (FBS) (Atlanta Biologicals, Norcross, GA), 100 units/ml penicillin G (Sigma), 100 μg/ml streptomycin (Sigma), and maintained in a 95% air/5% CO_2-humidified incubator at 37 °C. The cells were subcultured every 72 h. MC3T3-E1 cells, a preosteoblastic cell line (passage 10–20), were also cultured in α-MEM containing 10% FBS under the same conditions as the primary cells. MLO-Y4 osteocytes were cultured in α-MEM supplemented with 5% FBS and 5% calf serum.

Fluid Shear—Primary cells, MC3T3-E1 osteoblasts, and MLO-Y4 osteocytes were seeded at a density of 2,000/cm^2 and grown on 75 $\times$ 38-mm^2 glass slides (Fisher Scientific) coated with 10 $\mu g/cm^2$ collagen (BD Biosciences). Upon reaching 90% confluence (2–3 days), the cells were serum-starved for 24 h in 0.2% FBS-supplemented culture medium (the same medium used for flow). During the experiment, fluid flow was applied to the cell monolayer in a parallel plate flow chamber using a closed flow loop. This system subjected the cells to a steady laminar flow thus producing a 12 dynes/cm^2 FSS. The apparatus was maintained at 37 °C, and the medium was aerated with 95% air/5% CO_2 during experiment. In functional studies, the agonists were added immediately prior to flow, while the antagonists were applied to the cells for 30 min prior to flow. The cells were fluid-sheared for either 30 (for pore formation) or 15–60 min (for PGE_2 assay). Control groups were set under the same conditions without flow or drug treatments.

Agonists and Antagonists—To determine the functions of $P2X_7$ ion channel, several agonists and antagonists were used. BzATP (300 μM, which has been shown to have a high affinity for the $P2X_7R$ (33), was used to activate $P2X_7$ ion channel and pore formation. The $P2X_7R$-selective inhibitor, Brilliant Blue G (BBG) (1 μM), was used to block the $P2X_7$ ion channel and pore formation. To determine the roles of FSS-induced ATP release in activation of $P2X_7R$, apyrase (5 units/ml) was used. All the above reagents were purchased from Sigma. The $P2X_7$ antibody that binds to the extracellular portion of the receptor to inhibit activation was obtained from Alomone Laboratories.

Pore Formation Assay—Fluid shear stress-induced pore formation was determined by measuring cellular uptake of YO-PRO-1, molecular mass = 629 daltons; Molecular Probes, Eugene, OR) in primary cells as well as MC3T3-E1 cells. As described above, the cells were fluid sheared

for 30 min. After shear, the cells were rinsed once in PBS without Mg^{2+} and Ca^{2+} ions, which have been shown to inhibit pore formation (34). The YO-PRO-1 iodide dye (1 mM in Me_2SO) was diluted to a final concentration of 2 μM in PBS (without Mg^{2+} and Ca^{2+}) and then placed on the cells immediately and incubated for 10 min. Afterward, the cells were washed again with PBS without Mg^{2+} and Ca^{2+}. The stain-positive cells were observed under an UV-lighted microscope. YO-PRO-1-positive cells were normalized to total cells in the same vision field. The ratios of YO-PRO-1-positive cells over total cells were compared between different treatment groups, and a statistical difference was considered significant when p value was less than 0.05 (5% level). The pore formation assays were repeated three times for each of the experimental conditions.

Measurement of ATP—An ATP bioluminescence assay containing luciferin/luciferase reagent is used to detect ATP (ATP bioluminescence assay kit HS II, Roche Applied Science). This assay utilizes the conversion of D-luciferin by luciferase into oxyluciferin and light that requires ATP as a cofactor. The resultant luminescence, measured using a Monolight 3010 (Pharmingen), reflects ATP concentration. Media samples were taken 1 or 5 min after beginning fluid shear stress and immediately frozen at −80 °C for further analysis.

Prostaglandin E_2 Assay—Cells were subjected to fluid shear stress for either 15 or 60 min. After 60 min of fluid shear flow, 2 ml of 0.2% FBS α-MEM media was added onto the monolayer of cells and incubated for 30 min at 37 °C in the incubator. After 30 min, the conditioned media were collected for PGE_2 assay using a commercially available, competitive binding enzyme immunoassay kit (BioTrak, Amersham Biosciences). PGE_2 release to the conditioned media was normalized to total cell protein. The protein assay was accomplished by Amino Black method as used in Western blot.

Apoptosis Assay—To obtain a positive control for apoptosis, MC3T3-E1 cells were treated with TNF-α and cyclohexamide (CHX) for 6 h, then lysed for Western blot analysis (35). Together with this positive control, cell lysates from different treatment groups of FSS, BzATP, as well as static control were resolved through 10% SDS-PAGE and blotted with caspase-3 antibody (1:1,000, Cell Signaling, Beverly, MA) as described below.

Western Blot—Following treatment, cells were washed with cold PBS (1×), lysed with 2× sample buffer on ice, and immediately boiled for 5 min. The lysis buffer contained 150 mM NaCl, 26% glycerol (v/v), 1.5 mM $MgCl_2$, 0.2 mM EDTA, 0.5 mM dithiothreitol, 0.5 mM phenylmethylsulfonyl fluoride and buffered with 5 mM Na^+-HEPES (pH 7.9). The protein samples were centrifuged at 14,000 × g for 10 min at room temperature to remove cellular debris and then quantified using the Amido Black method. Whole cell lysate (20 μg) and a prestained molecular weight marker (Bio-Rad) were boiled for 5 min and separated by 10% SDS-polyacrylamide gel electrophoresis and electrotransferred to a nitrocellulose membrane. The membrane was blocked in Tris-buffered saline containing 5% nonfat dry milk and 0.1% Tween 20 (TBST) and incubated with 1 μg/ml (1:250 in blocking buffer) rabbit anti-P2X$_7$R antibody (Calbiochem) overnight at 4 °C. The membranes were then washed three times with TBST and incubated with goat anti-rabbit IgG hydroperoxidase-conjugated secondary antibodies (1:5,000 in blocking buffer) for 1 h at room temperature. After washing with TBST, immunodetection was accomplished using the ECL method (Fuji machine).

Statistical Analysis—All the data were expressed as mean ± S.E. Differences between parameters in the loaded (right) and nonloaded (left) ulnae were tested using a paired t test. Dose response to different load magnitudes and mechanical strain within each gender WT or KO mice were tested for significance with least square regression. Differences in slope and x intercept (bone formation *versus* mechanical strain) between same gender WT and KO mice were tested for significance by analysis of covariance. For all tests, $\alpha = 0.05$. In cellular studies, Western blots were made from either three separate isolations for primary cells or three different passages of cell lines. Significance was established from densitometry measurements using Dunnett's comparison to the static controls or Bonferroni *post hoc* test for multiple comparisons.

RESULTS

P2X$_7$R Null Mice Were Grossly Normal—In general, P2X$_7$R KO mice appeared normal. At 18 weeks of age, body weights for male KO mice were higher (+5%; $p = 0.02$) than male WT controls. There were no differences in body weights between KO and WT female mice ($p = 0.62$). No differences in femoral length were found between KO and WT in female ($p = 0.63$) or male ($p = 0.62$) mice.

The Osteogenic Response to Mechanical Loading Was Suppressed in P2X$_7$R Null Mice—We hypothesized that the long bones of P2X$_7$R null mice would be less responsive to mechanical loading. A verified experimental approach involving axial loading of the mouse ulna induced new bone formation, mainly at the medial and lateral quadrants of the periosteal surface (Fig. 1). The load-induced bone was lamellar based on the observation under polarized light microscope. Bone formation parameters rMS/BS, rMAR, and rBFR/BS were increased in a magnitude-dependent manner with mechanical loading. All bone formation parameters were significantly greater in WT mice than KO mice ($p < 0.01$). Of the bone formation parameters rBFR/BS best represents the new bone formation rate, which was closely correlated with peak mechanical strain calculated at the midshaft ulna (Fig. 2). Analysis of the correlations between mechanical strain and rBFR/BS revealed significant differences between WT and KO female mice ($p < 0.01$; Fig. 2*A*). Sensitivity to loading (the slope of rBFR/BS *versus* strain) in female KO mice was reduced by 61% compared with female WT mice, demonstrating that female WT mice exhibited significantly higher rBFR/BS per unit mechanical strain than female KO mice. Sensitivity to mechanical loading in male KO mice was reduced by 73% compared with male WT mice ($p < 0.0001$; Fig. 2*B*). In addition, the x intercept of the dose-response curve for the male KO mice was about 31% greater ($p = 0.02$) in comparison with male WT mice, indicating that more mechanical strain was required to initiate a response in KO mice.

ATP Release Is Not Suppressed in Osteoblasts from P2X$_7$R Null Mice—To study the role of P2X$_7$R in osteoblastic responsiveness to mechanical loading, we completed a series of experiments using cultured bone cells from newborn mouse calvaria osteoblasts. Western blot analysis revealed that the P2X$_7$R receptor was present in WT but not KO cells, whereas MC3T3-E1 osteoblasts and MLO-Y4 osteocytes expressed high levels of P2X$_7$R (Fig. 3). We have shown that FSS produces a 10-fold increase in ATP release in MC3T3-E1 osteoblasts within 1 min of the onset of FSS (36). When primary osteoblasts from WT mice were subjected to steady laminar fluid flow at 12 dynes/cm^2 FSS, release of ATP was also observed within 1 min. Primary bone cells from KO mice released similar amounts of ATP compared with WT cells (Fig. 4).

P2X$_7$R Null Mutation Eliminates Membrane Pore Formation and Prostaglandin Release after a Mechanical Stimulus—Activation of the P2X$_7$R has been linked with formation of pores in the cell membrane, capable of conducting large molecules (37). To examine whether activation of P2X$_7$R induced pore formation, we measured uptake of YO-PRO-1, a 629-dalton protein that becomes fluorescent when it binds to nucleic acids, in WT and KO primary bone cells and MC3T3-E1 osteoblasts. FSS induced P2X$_7$R-mediated pore formation in WT and

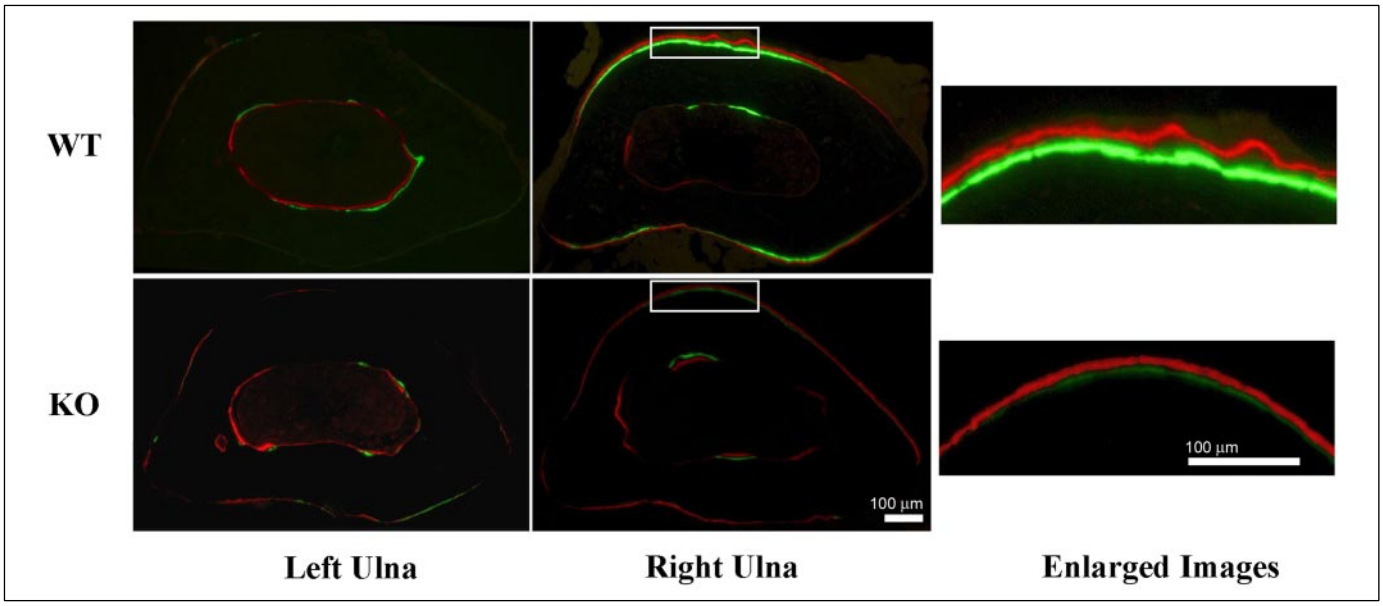

FIGURE 1. **Periosteal bone formation at the ulnar midshaft was increased with mechanical loading that induces 2,500-μ strain.** Mechanical loading of the right ulna activated the formerly quiescent medial and lateral periosteal surfaces, as illustrated by the double fluorochrome labeling (*bright bands* near the bone surface). Bone formation induced by loading exhibited lamellar organization. The responses in WT mice were more robust (illustrated by the clear double labels) compared with KO mice in which double labels are hard to discern. Note the lack of response in the caudal and cranial periosteal surfaces, which straddle the neutral bending axis, and are consequently subjected to very low strains.

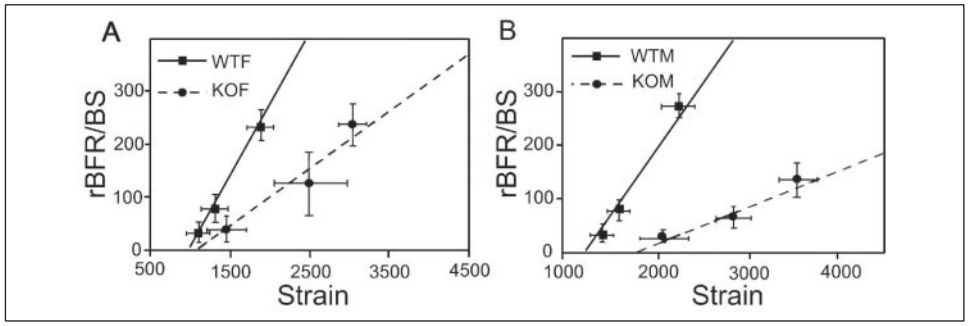

FIGURE 2. **Relative (right minus left) bone formation rate was normalized to peak mechanical strain.** *A*, female P2X$_7$R knock-out mice exhibited lower sensitivity than female wild type mice; *B*, male P2X$_7$R knock-out mice exhibited a higher osteogenic threshold and a lower rBFR/BA *versus* strain slope (lower sensitivity).

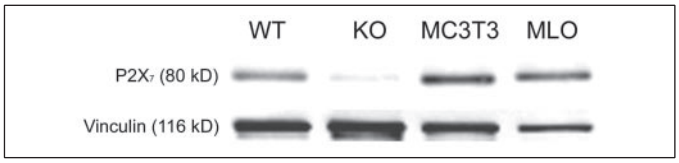

FIGURE 3. **Western blot of P2X$_7$R for calvarial osteoblasts from WT and KO mice, MC3T3-E1 osteoblasts, and MLO-Y4 osteocytes.**

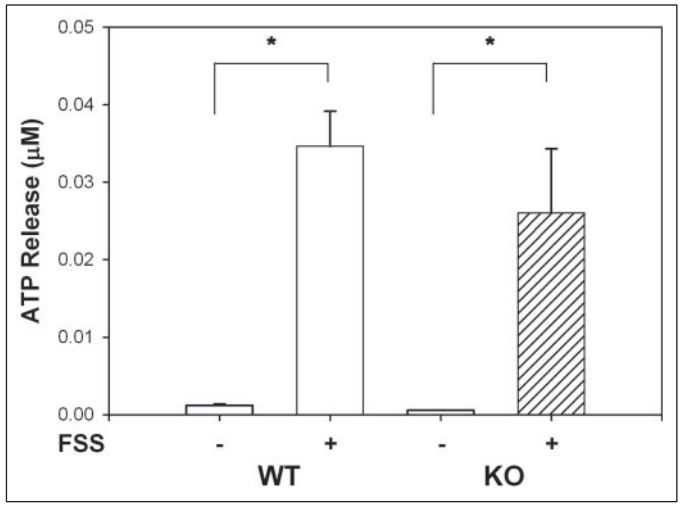

FIGURE 4. **Release of ATP was observed within 1 min following steady laminar fluid flow at 12 dynes/cm^2 FSS.** Bone cells from KO mice released similar amounts of ATP compared with WT cells.

MC3T3-E1 osteoblasts and MLO-Y4 osteocytes but not in KO osteoblasts (Fig. 5*A*). Activation of P2X$_7$R with BzATP also produced pore formation in MC3T3-E1 and WT osteoblasts and MLO-Y4 osteocytes, but not in KO osteoblasts (Fig. 5*B*). When apyrase was added to the flow media to degrade ATP, pore formation was almost completely inhibited in MC3T3-E1 and MLO-Y4 cells (Fig. 6).

To begin to determine the cellular function of the P2X$_7$R, we examined the effects of P2X$_7$R inhibition on prostaglandin release in MC3T3-E1 and MLO-Y4 cells. FSS significantly increased PGE_2 release in MC3T3-E1 osteoblasts and MLO-Y4 osteocytes. The P2X$_7$R blocker BBG inhibited PGE_2 release in osteoblasts in a dose-dependent manner (Fig. 7*A*). Addition of a P2X$_7$R antibody to MC3T3-E1 osteoblasts or MLO-Y4 osteocytes also significantly suppressed PGE_2 release to a similar degree in each cell line (Fig. 7*B*), indicating that prostaglandin release is dependent on ATP signaling through P2X$_7$R. Addition of the P2X$_7$R agonist, BzATP, to MC3T3-E1 and MLO-Y4 cells in the absence of FSS increased the release of PGE_2 (Fig. 7*C*), further suggesting that signaling through the P2X$_7$R leads to PGE_2 release in osteoblasts and osteocytes. FSS significantly increased PGE_2 release in WT cells ($p < 0.0001$) but had no significant effect on PGE_2 release in P2X$_7$R KO cells

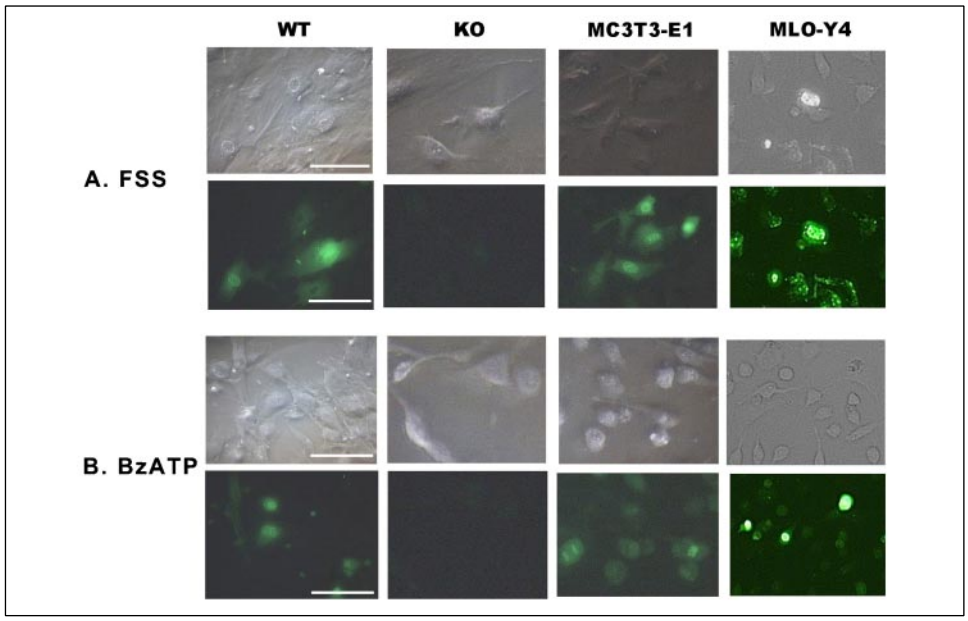

FIGURE 5. *A*, 30 min of FSS induced membrane pore formation, as determined by measuring cellular uptake of YO-PRO-1 (molecular mass = 630 daltons) in WT and MC3T3-E1 osteoblasts and MLO-Y4 osteocytes but not in KO osteoblasts. *B*, the P2X$_7$R agonist BzATP induced pore formation in WT and MC3T3-E1 osteoblasts and MLO-Y4 osteocytes but not in KO osteoblasts. *Scale bars* represent 20 μm.

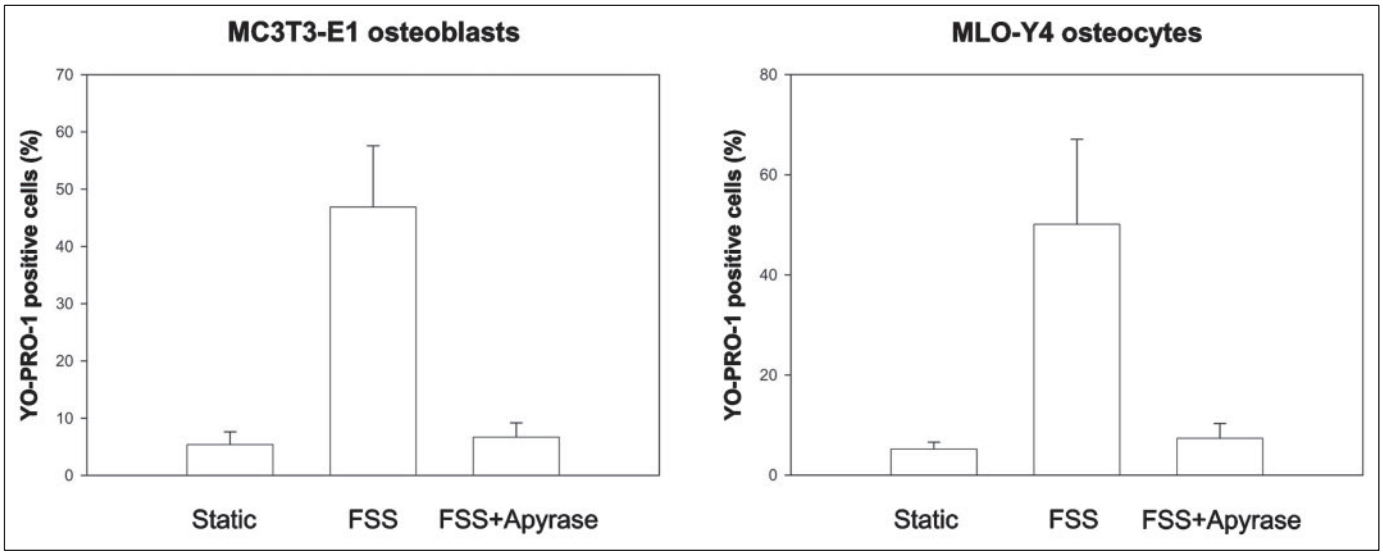

FIGURE 6. **MC3T3-E1 osteoblasts and MLO-Y4 osteocytes were subjected to FSS for 30 min and incubated with YO-PRO-1 (1 μM) for 10 min.** FSS induced pore formation and adding apyrase, which rapidly hydrolyzes ATP, to the media blocked pore formation.

($p = 0.9$) (Fig. 8), demonstrating that the P2X$_7$R is required for mechanically induced PGE_2 release in osteoblasts.

P2X$_7$R Activation Was Not Associated with Increased Osteoblast Apoptosis—Increased pore formation in the cell membrane has been associated with an increase in cellular apoptosis (38). To determine whether pore formation induced by P2X$_7$R activation increased apoptosis in bone cells, we examined the activation of caspase-3 in MC3T3-E1 MC3T3-E1 osteoblasts subjected to either fluid shear or BzATP. Both of these treatments were shown previously to increase membrane pore formation. As a positive control, MC3T3-E1 osteoblasts were treated with TNF-α and CHX for 6 h (35). Western analysis demonstrated that TNF-α and CHX treated osteoblasts exhibited both an inactive form of caspase-3 (34 kDa) and an active form (17 kDa), which is believed to play a key role in apoptosis (Fig. 9). However, only the 34-kDa inactive form of caspase-3 was observed in the FSS, BzATP, and static control groups indicating that, whereas these treatments caused P2X$_7$R mediated pore formation, neither FSS nor BzATP increased osteoblast apoptosis. We then examined cell mass (measured as total cell protein) in primary cultures of osteoblasts from WT or P2X$_7$R KO calvaria. Total cell protein did not differ ($p = 0.54$) for nine samples from WT cells compared with seven samples from KO cells. We conclude that activation of P2X$_7$R did not increase osteoblast apoptosis in MC3T3-E1 osteoblasts, and cell growth was similar for WT and KO cells in culture suggesting no gross differences in cellular apoptosis.

DISCUSSION

ATP is an early mediator of mechanotransduction in osteoblasts that is released from cells within 1 min after applying mechanical loading (36). ATP initiates intracellular calcium release in osteoblasts through P2Y receptor pathways, which has been the main focus of several previous studies (15–16). However, our results suggest that a novel pathway involving P2X$_7$R activation is a major contributor to osteoblast mechanotransduction. This pathway culminates in PG release that promotes osteogenesis. Indeed, as much as 73% of the osteogenic response to loading *in vivo* appears to be linked to the P2X$_7$R. Previous studies have shown that 50–90% of mechanically induced osteogenesis can be

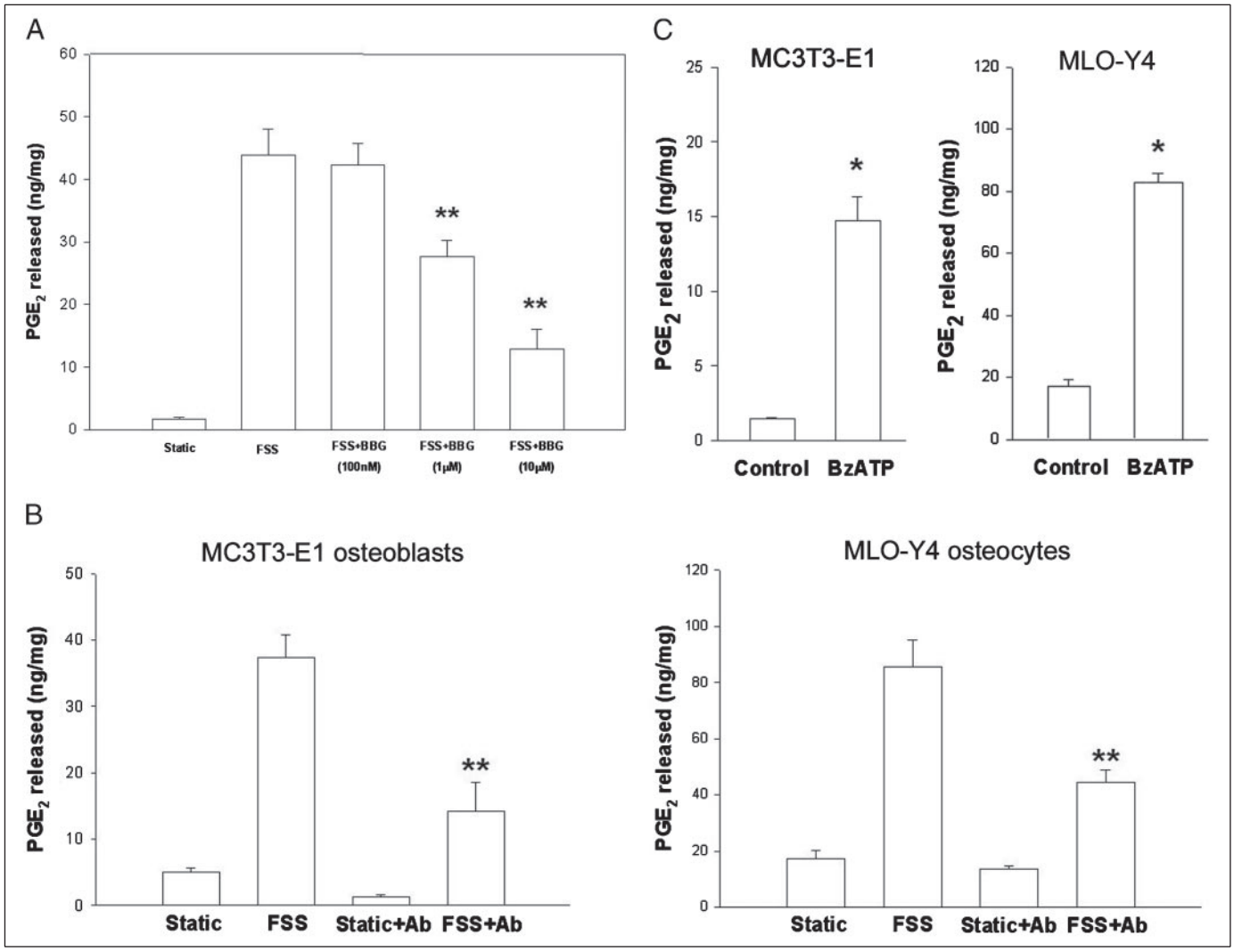

FIGURE 7. *A*, the P2X$_7$R antagonist BBG reduced PGE_2 release from MC3T3-E1 osteoblasts in a dose-dependent manner. *B*, the P2X$_7$R antibody (extracellular) significantly reduced flow-enhanced PGE_2 release from MC3T3-E1 osteoblasts or MLO-Y4 osteocytes. *C*, the P2X$_7$R agonist BzATP increased PGE_2 release from MC3T3-E1 osteoblasts and MLO-Y4 osteocytes. *, significantly greater than negative control; **, significantly less than positive control.

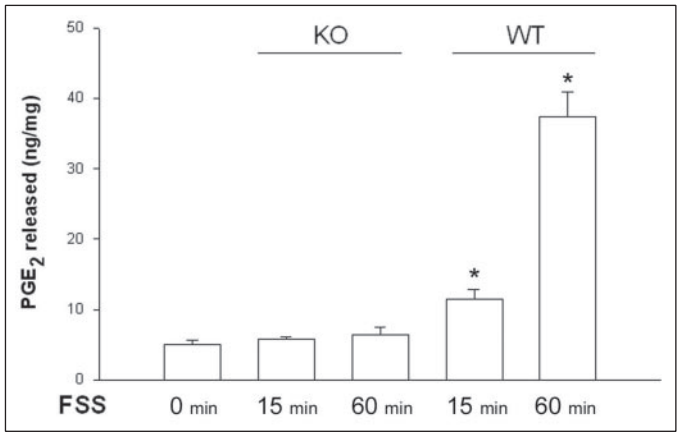

FIGURE 8. **PGE_2 release was significantly increased after 15 and 60 min of FSS ($p = 0.0001$) in WT cells, but PGE_2 release in KO cells was not significantly increased by FSS at either time point ($p = 0.9$).** *, significantly greater than negative control.

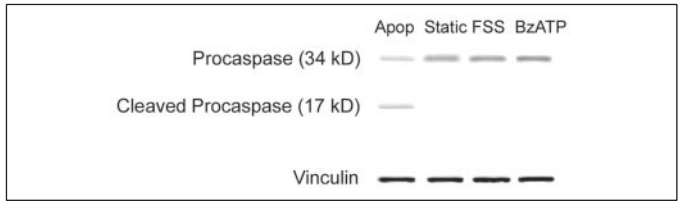

FIGURE 9. **As a positive control, MC3T3-E1 osteoblasts treated with TNF-α and cyclohexamide (*Apop*) possessed not only an inactive for of caspase-3 (*34 kD*), but also an active form of caspase-3 (*17 kD*), demonstrating that apoptosis was induced.** However, compared with the static control group, neither FSS nor P2X$_7$R agonist BzATP induced the active form of caspase-3 (*17kD*).

suppressed using blockers of prostaglandin synthesis (39–41), demonstrating the importance of this pathway for bone formation.

Our results indicate that P2X$_7$R KO mice are less sensitive to mechanical loading compared with WT mice. The lower mechanosensitivity in P2X$_7$R KO mice can be demonstrated by two independent parameters. First, the increase in bone formation per unit increase mechanical strain was significantly less in KO mice than that in WT mice. Thus, equal increases in mechanical strain resulted in less new bone formation in KO mice than WT mice. Second, the osteogenic threshold in male KO mice was significantly greater than male WT mice, indicating that a higher strain was necessary to initiate an anabolic response. Interestingly, the osteogenic thresholds between female KO and WT mice were not significantly different, suggesting that the effect of the P2X$_7$R null mutation was more severe in male than female mice.

These findings are consistent with the bone phenotypes in P2X$_7$R KO mice, as the periosteal bone formation rate was significantly less in male compared with female mice (29). The mechanism for this difference is unclear, but one study reported that 17β-estradiol inhibits P2X$_7$R activation (42). These data suggest an interaction between sex steroids and P2X$_7$R signaling.

Fluid shear stress increased the formation of nonselective aqueous pores in the plasma membrane of osteoblasts and osteocytes through activation of the P2X$_7$R. Pore formation could be mimicked by P2X$_7$R agonists, such as BzATP, and could be blocked by P2X$_7$R antagonists, such as P2X$_7$R antibody. It is been reported that prolonged P2X$_7$R activation causes apoptosis in immune cells (38) and can induce apoptosis in osteoblasts (38, 43). However, we did not find an increase in apoptosis in MC3T3-E1 osteoblasts subjected to FSS, even though FSS caused pore formation in over 30% of the cells, nor did the P2X$_7$R agonist BzATP induce apoptosis in osteoblasts. Others have shown that FSS protects osteoblastic cells against TNF-α induced apoptosis (35) furthering the argument that mechanical stimuli suppress, rather than increase, apoptosis. It is unclear what physiological role the FSS-induced membrane pores play yet they do not appear to initiate apoptotic pathways.

Fluid shear induced pore formation in cell membranes of osteoblasts and MLO-Y4 osteocytes. This observation is consistent with another study in which pore formation in MLO-Y4 cells was seen after fluid shear (44). It has been proposed that membrane pores form by opening connexin 43 (Cx43) hemichannels. While this mechanism has some experimental support (44), our data suggest that the membrane pore formation is mediated by ATP and the major mechanism is the P2X$_7$R. We observed pore formation after treatment with the P2X$_7$R agonist BzATP and pore formation in osteoblasts, and MLO-Y4 osteocytes was blocked with apyrase, which hydrolyzes extracellular ATP thus interrupting its signaling. Others have suggested that Cx43 and P2X$_7$R might have interacting functions (45). In peritoneal macrophages, Cx43 and P2X$_7$R are co-localized at the cell membrane. However, we were not able to demonstrate membrane co-localization of Cx43 and P2X$_7$R in MLO-Y4 osteocytes.[4]

When subjected to mechanical loading, osteoblasts from P2X$_7$R KO mice did not release prostaglandin E$_2$. PGE$_2$ is an anabolic factor in bone (7), and the lack of PGE$_2$ response in KO cells is probably the cause of the suppressed bone formation response to loading observed in P2X$_7$R KO mice. Using a cell culture assay of bone formation, others have shown that primary osteoblasts from P2X$_7$R KO mice do not form mineralized nodules as well as WT osteoblasts (46). Moreover, nodule formation has been shown to be enhanced by the P2X$_7$R agonist BzATP and suppressed by blockade of prostaglandin synthesis with ibuprofen (46). These findings support our supposition that P2X$_7$R mediates new bone formation through release of prostaglandins.

It has been shown previously that P2X$_7$R forms a complex with several putative mechanotransduction proteins such as RPTP or α-actinin, so the genetic mutation of P2X$_7$R could have disrupted the mechanotranduction complex and interfered with other related mechanotransduction pathways. However, since we were able to suppress PGE$_2$ release in osteoblasts and osteocytes using a neutralizing antibody for P2X$_7$R, our data suggest that blockade of P2X$_7$R is effective for suppressing mechanotransduction when the P2X$_7$R and associated proteins are intact.

Although the absence of a functional P2X$_7$R resulted in significantly lower sensitivity to loading, the response was not completely abolished.

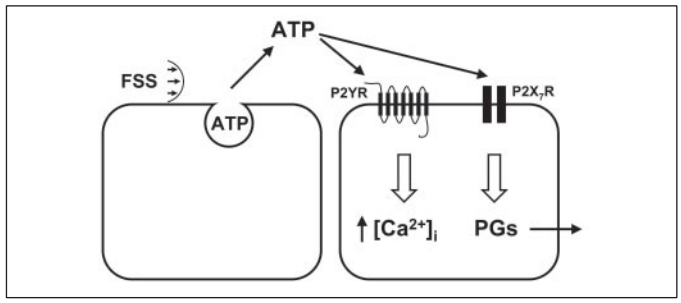

FIGURE 10. **Release of ATP after FSS in osteoblasts causes signaling through two pathways: P2YR, resulting in intracellular calcium mobilization, and P2X$_7$R, resulting in prostaglandin release.**

Thus there is the possibility that other P2 receptors are also involved in osteoblastic response to loading. For instance, one previous study demonstrated that P2Y$_2$R antisense oligodexoxynucleotides decreased the percentage of MC3T3-E1 osteoblastic cells responding to fluid flow with an increase intracellular calcium [Ca^{2+}]$_i$ (16). Others (15, 16) have shown that ATP can induce [Ca^{2+}]$_i$ mobilization in osteoblasts. In endothelial cells, the addition of apyrase, which rapidly hydrolyzes 5′-nucleotide triphosphates to monophosphates, prevents shear stress induced Ca^{2+} influx (11). This ATP-mediated [Ca^{2+}]$_i$ pathway appears to be independent of P2X signaling (16) suggesting that ATP works through two distinct signaling pathways during osteoblast mechanotransduction: 1) P2X activation leading to PG release and 2) P2Y activation and [Ca^{2+}]$_i$ mobilization (Fig. 10). Previous studies suggest that these two pathways are largely independent (47). The present study demonstrates that the majority of the osteogenic response is linked to nucleotide signaling through P2X$_7$R and subsequent PG release from bone cells.

P2X$_7$R is expressed not only in osteoblasts but also in active osteoclasts and osteoclast precursors (48). Signaling through P2X$_7$R plays a role in osteoclast formation (49, 50) and activation (51). It has been proposed that mechanical loading acts in part on osteoclasts via the P2X$_7$R (33). This interesting possibility was not tested in the current study. For our experiments, we applied mechanical loading to the ulna of adult mice. In this model, the surfaces of the bone were largely quiescent with minimal bone formation and no bone resorption. After mechanical loading of the mouse ulna, osteoblasts were recruited to the bone surfaces and new bone formation was observed but the histological sections were free of osteoclasts. Consequently, our experiments using adult mice allowed us to study the specific effect of mechanical loading on bone formation without indirect effects mediated by osteoclasts. Others (52) have shown that the ulnae of young, growing rodents demonstrate active bone resorption, in addition to bone formation, and in this model mechanical loading suppresses osteoclast activity. Whether the P2X$_7$R mediates the loading effect on osteoclasts remains to be determined.

The linkage between the P2X$_7$R and osteogenesis provides possible therapeutic options for improving fracture healing and for skeletal diseases. Since the P2X$_7$R plays a significant role in mechanotransduction, agonists for this receptor may induce the more bone formation where mechanical stresses are highest. This provides a means for optimizing skeletal structure by placing bone only where it is most needed. Our previous study showed that mechanical loading of rat forelimbs can improve bone strength by almost 2-fold, even with only modest (5%) increases in bone mineral density (1). Consequently, selective targeting the P2X$_7$R may provide an efficient means for strengthening bone to treat diseases of bone fragility like osteoporosis or osteogenesis imperfecta. Also several PGs, particularly PGE$_2$, substantially increase bone

[4] A. B. Castillo and C. H. Turner, unpublished data.

formation and improve bone strength when administered to rats (7, 53). Since the P2X$_7$R is linked to load-induced release of PGE_2, manipulation of this receptor may provide a means to augment PGE_2 release locally. This strategy might prove useful for accelerating fracture healing or for improving bone regeneration around implants.

REFERENCES

1. Robling, A. G., Hinant, F. M., Burr, D. B., and Turner, C. H. (2002) *J. Bone Miner Res.* **17,** 1545–1554
2. Bakker, A. D., Klein-Nulend, J., and Burger, E. H. (2003) *Biochem. Biophys. Res. Commun.* **305,** 677–683
3. Klein-Nulend, J., Semeins, C. M., and Burger, E. H. (1996) *J. Cell Physiol.* **168,** 1–7
4. Perrone, C. E., Fenwick-Smith, D., and Vandenburgh, H. H. (1995) *J. Biol. Chem.* **270,** 2099–2106
5. Pitsillides, A. A., Rawlinson, S. C., Suswillo, R. F., Bourrin, S., Zaman, G., and Lanyon, L. E. (1995) *FASEB J.* **9,** 1614–1622
6. Chow, J. W. (2000) *Exerc. Sport Sci. Rev.* **28,** 185–188
7. Jee, W. S., and Ma, Y. F. (1997) *Bone* (*N. Y.*) **21,** 297–304
8. Graff, R. D., Lazarowski, E. R., Banes, A. J., and Lee, G. M. (2000) *Arthritis Rheum.* **43,** 1571–1579
9. Grierson, J. P., and Meldolesi, J. (1995) *J. Biol. Chem.* **270,** 4451–4456
10. Shen, J., Luscinskas, F. W., Connolly, A., Dewey, C. F., Jr., and Gimbrone, M. A., Jr. (1992) *Am. J. Physiol.* **262,** C384–C390
11. Yamamoto, K., Sokabe, T., Ohura, N., Nakatsuka, H., Kamiya, A., and Ando, J. (2003) *Am. J. Physiol.* **285,** H793–H803
12. Buckley, K. A., Golding, S. L., Rice, J. M., Dillon, J. P., and Gallagher, J. A. (2003) *FASEB J.* **17,** 1401–1410
13. Romanello, M., Pani, B., Bicego, M., and D'Andrea, P. (2001) *Biochem. Biophys. Res. Commun.* **289,** 1275–1281
14. Bowler, W. B., Buckley, K. A., Gartland, A., Hipskind, R. A., Bilbe, G., and Gallagher, J. A. (2001) *Bone* **28,** 507–512
15. Jorgensen, N. R., Geist, S. T., Civitelli, R., and Steinberg, T. H. (1997) *J. Cell Biol.* **139,** 497–506
16. You, J., Jacobs, C. R., Steinberg, T. H., and Donahue, H. J. (2002) *J. Biol. Chem.* **277,** 48724–48729
17. Brambilla, R., and Abbracchio, M. P. (2001) *Ann. N. Y. Acad. Sci.* **939,** 54–62
18. Koolpe, M., Pearson, D., and Benton, H. P. (1999) *Arthritis Rheum.* **42,** 258–267
19. Suzuki, A., Kotoyori, J., Oiso, Y., and Kozawa, O. (1993) *Cell Adhes. Commun.* **1,** 113–118
20. Bowler, W. B., Dixon, C. J., Halleux, C., Maier, R., Bilbe, G., Fraser, W. D., Gallagher, J. A., and Hipskind, R. A. (1999) *J. Biol. Chem.* **274,** 14315–14324
21. North, R. A. (2002) *Physiol. Rev.* **82,** 1013–1067
22. Di Virgilio, F., Chiozzi, P., Ferrari, D., Falzoni, S., Sanz, J. M., Morelli, A., Torboli, M., Bolognesi, G., and Baricordi, O. R. (2001) *Blood* **97,** 587–600
23. Surprenant, A., Rassendren, F., Kawashima, E., North, R. A., and Buell, G. (1996) *Science* **272,** 735–738
24. Ferrari, D., Chiozzi, P., Falzoni, S., Dal Susino, M., Melchiorri, L., Baricordi, O. R., and Di Virgilio, F. (1997) *J. Immunol.* **159,** 1451–1458
25. Ferrari, D., Los, M., Bauer, M. K., Vandenabeele, P., Wesselborg, S., and Schulze-Osthoff, K. (1999) *FEBS Lett.* **447,** 71–75
26. Kim, M., Jiang, L. H., Wilson, H. L., North, R. A., and Surprenant, A. (2001) *EMBO J.* **20,** 6347–6358
27. von Wichert, G., Jiang, G., Kostic, A., De Vos, K., Sap, J., and Sheetz, M. P. (2003) *J. Cell Biol.* **161,** 143–153
28. Pavalko, F. M., Chen, N. X., Turner, C. H., Burr, D. B., Atkinson, S., Hsieh, Y. F., Qiu, J., and Duncan, R. L. (1998) *Am. J. Physiol.* **275,** C1591–C1601
29. Ke, H. Z., Qi, H., Weidema, A. F., Zhang, Q., Panupinthu, N., Crawford, D. T., Grasser, W. A., Paralkar, V. M., Li, M., Audoly, L. P., Gabel, C. A., Jee, W. S., Dixon, S. J., Sims, S. M., and Thompson, D. D. (2003) *Mol. Endocrinol.* **17,** 1356–1367
30. Uhthoff, H. K., and Jaworski, Z. F. (1978) *J. Bone Joint Surg. Br.* **60-B,** 420–429
31. Solle, M., Labasi, J., Perregaux, D. G., Stam, E., Petrushova, N., Koller, B. H., Griffiths, R. J., and Gabel, C. A. (2001) *J. Biol. Chem.* **276,** 125–132
32. Robling, A. G., and Turner, C. H. (2002) *Bone* **31,** 562–569
33. Naemsch, L. N., Dixon, S. J., and Sims, S. M. (2001) *J. Biol. Chem.* **276,** 39107–39114
34. Virginio, C., Church, D., North, R. A., and Surprenant, A. (1997) *Neuropharmacology* **36,** 1285–1294
35. Pavalko, F. M., Gerard, R. L., Ponik, S. M., Gallagher, P. J., Jin, Y., and Norvell, S. M. (2003) *J. Cell. Physiol.* **194,** 194–205
36. Genetos, D. C., Geist, D. J., Liu, D., Donahue, H. J., and Duncan, R. L. (2005) *J. Bone Miner. Res.* **20,** 41–49
37. Rassendren, F., Buell, G., Newbolt, A., North, R. A., and Surprenant, A. (1997) *EMBO J.* **16,** 3446–3454
38. Wiley, J. S., Dao-Ung, L. P., Gu, B. J., Sluyter, R., Shemon, A. N., Li, C., Taper, J., Gallo, J., and Manoharan, A. (2002) *Lancet* **359,** 1114–1119
39. Chambers, T. J., Chow, J. W., Fox, S.W, Jagger, C. J., and Lean, J. M. (1997) *Adv. Exp. Med. Biol.* **433,** 295–298
40. Forwood, M. R. (1996) *J. Bone Miner. Res.* **11,** 1688–1693
41. Li, J., Burr, D. B., and Turner, C. H. (2002) *Calcif. Tissue Int.* **70,** 320–329
42. Cario-Toumaniantz, C., Loirand, G., Ferrier, L., and Pacaud, P. (1998) *J. Physiol.* **508,** 659–666
43. Gartland, A., Hipskind, R. A., Gallagher, J. A., and Bowler, W. B. (2001) *J. Bone Miner. Res.* **16,** 846–856
44. Cherian, P. P., Siller-Jackson, A. J., Gu, S., Wang, X., Bonewald, L. F., Sprague, E., Jiang, J. X. (2005) *Mol. Biol. Cell* **16,** 3100–3106
45. Fortes, S. A., Pecora, I. L., Persechini, P. M., Hurtado, S., Costa,V., Coutinho-Silva, R., Bragg, M. B., Silva-Filho, F. C., Bisaggio, R. C., De Farias, F. P., Scemes, E., De Carvalho, A. C., and Goldenberg, R. C. (2004) *J. Cell Sci.* **117,** 4717–4726
46. Panupinthu, N., Ke, H. Z., Sims, S. M., and Dixon, S. J. (2005) *J. Bone Miner. Res.* **20,** Suppl. 1, S248
47. Saunders, M. M., You, J., Zhou, Z., Li, Z., Yellowley, C. E., Kunze, E. L., Jacobs, C. R., and Donahue, H. J. (2003) *Bone* **32,** 350–356
48. Gartland, A., Buckley, K. A., Hipskind, R. A., Bowler, W. B., Gallagher, J. A. (2003) *Crit. Rev. Eukaryotic Gene Expression* **13,** 237–242
49. Gartland, A., Buckley, K. A., Bowler, W. B., Gallagher, J. A. (2003) *Calcif. Tissue Int.* **73,** 361–369
50. Hiken, J. F., and Steinberg, T. H. (2004) *Am. J. Physiol.* **287,** C403–C412
51. Korcok, J., Raimundo, L. N., Ke, H. Z., Sims, S. M., Dixon, S. J. (2004) *J. Bone Miner. Res.* **19,** 642–651
52. Hillam, R. A., Skerry, T. M. (1995) *J. Bone Miner. Res.* **10,** 683–689
53. Ke, H. Z., Shen, V. W., Qi, H., Crawford, D. T., Wu, D. D., Liang, X. G., Chidsey-Frink, K. L., Pirie, C. M., Simmons, H. A., and Thompson, D. D. (1998) *Bone* **23,** 249–255